PNAS

Supplementary Information for

LRBA is essential for urinary concentration and body water homeostasis

Yu Hara, Fumiaki Ando*, Daisuke Oikawa, Koichiro Ichimura, Hideki Yanagawa, Yuriko Sakamaki, Azuma Nanamatsu, Tamami Fujiki, Shuichi Mori, Soichiro Suzuki, Naofumi Yui, Shintaro Mandai, Koichiro Susa, Takayasu Mori, Eisei Sohara, Tatemitsu Rai, Mikiko Takahashi, Sei Sasaki, Hiroyuki Kagechika, Fuminori Tokunaga & Shinichi Uchida*

* Fumiaki Ando
Email: fandkidc@tmd.ac.jp
* Shinichi Uchida
Email: suchida.kid@tmd.ac.jp

This PDF file includes:

Supplementary text
Figures S1 to S13
Table S1

Supplementary text

Materials and Methods

Study approvals.
All animal studies were performed in accordance with the guidelines for animal research of Tokyo Medical and Dental University. The study protocol was approved by the Animal Care and Use Committee of Tokyo Medical and Dental University (approval number: A2021-120C).

Animals.
C57BL/6J mice were purchased from CLEA JAPAN (Tokyo, Japan). Female mice were used for experiments at 10-weeks-old. All mice were maintained under standard lightning conditions (12 h: 12 h light-dark cycle).

Generation and breeding of *Lrba* knockout mice.
Lrba knockout mice were generated in C57/BL6J zygotes using the CRISPR/Cas9 genome-editing system. The sgRNA sequence targeting the second exon of *Lrba* was 5′- CCG GGG CTC CCC ATC AGG GGC AT-3′. A 14 base-pair deletion mutation in exon2 was generated (Figure 1G). This mutation led to a frameshift in *Lrba* transcript, resulting in the truncation of the LRBA protein. This mutant strain was backcrossed to C57BL/6J for 10 generations to remove potential off-target variants. Genotypes were confirmed by Sanger sequencing with the following primers: *Lrba*-Forward, 5′-TGC CCT TAG TAA CTT ATT TG-3′ and *Lrba*-Reverse, 5′-AAC TTA CAT TAG CTC CCA AG-3′. Two $Lrba^{+/-}$ mice were crossed, generating WT, $Lrba^{+/-}$, and $Lrba^{-/-}$ mice with the same background.

Measurement of urine osmolality, urine output, and water intake.
Mice were kept individually in metabolic cages (KN-650-MM, Natsume Seisakusho, Tokyo, Japan) for 24 h with free access to food and water for urine osmolality, urine output, and water intake measurements. Urine osmolality was measured with a Fiske One-ten Osmometer (John Morris Scientific Pty Ltd., Chatswood, NSW, Australia).

Administration of water, dDAVP, and tolvaptan.
Mice received an acute water load equivalent to 3% of their body weight by oral gavage without access to food or water for 2 h (1). dDAVP (0.4 μg/kg) (Sigma-Aldrich) was intraperitoneally injected for 1 h (37). Tolvaptan (25 mg/kg/day) (LKT Laboratories, Inc., St. Paul, MN, USA) or vehicle (Dimethyl sulfoxide (DMSO); Sigma-Aldrich) was subcutaneously injected using osmotic minipumps (Alzet model 1003D; ALZA Corporation, Cupertino, CA, USA) as previously described (37).

Administration of LiCl
Mice received a control diet or a diet containing 0.2% LiCl (Sigma-Aldrich Corporation, St. Louis, MO, USA) for 21days.

Dehydration test.
WT, $Lrba^{+/-}$, and $Lrba^{-/-}$ mice were individually housed in standard cages and allowed free access to tap water. At the beginning of the exam, the water bottles were removed. After 12 h of water deprivation, the test was terminated because of 15% weight loss in $Lrba^{-/-}$ mice. Urine osmolality and body weight were measured at the beginning and end of the experiments.

Measurement of serum immunoglobulin and creatine levels.
Blood was obtained from the venous plexus near the mandible under anesthesia. Serum immunoglobulin levels were analyzed using IgG Mouse ELISA kit (#5010-1, Life Diagnostics, Inc.), IgA Mouse ELISA kit (#5016-1, Life Diagnostics, Inc., West Chester, PA, USA), and IgM Mouse ELISA kit (#5015-1, Life Diagnostics, Inc.). Serum creatinine levels were measured by SRL, Inc., a commercial laboratory in Tokyo, Japan.

Measurement of plasma vasopressin levels.
WT and *Lrba*$^{-/-}$ mice were allowed free access to tap water. Blood was obtained from the venous plexus near the mandible and collected into tubes containing ethylenediaminetetraacetic acid (EDTA). Plasma vasopressin concentrations were analyzed by the radioimmunoassay method at SRL, Inc., a commercial laboratory in Tokyo, Japan.

Densitometric analysis of urinary albumin.
Urine was collected for 24 hours using metabolic cages. Urine samples were denatured with SDS sample buffer after normalizing to urinary creatinine concentration. Urinary creatinine concentration was measured by LabAssay™ Creatinine (FUJIFILM Wako Pure Chemical, Osaka, Japan) according to the manufacturer's instructions. Urinary albumin was quantified by Western blot analysis. As a loading control, Coomassie brilliant blue staining was conducted using Bullet CBB Stain One (Nacalai Tesque, Kyoto, Japan) according to the manufacturer's procedure.

Quantification of urinary albumin.
Urine was collected for 24 hours using metabolic cages. Urinary albumin concentrations were analyzed at SRL, Inc., a commercial laboratory in Tokyo, Japan. Albumin excretion was obtained by multiplication of the urinary albumin concentration by 24-hour urine output.

Cell culture and transfections.
mpkCCDcl4 cells, a gift from Alain Vandewalle, were cultured as previously described (2). The mpkCCD cells were seeded and grown on semipermeable filters (Transwell®, 0.4-μm pore size; Corning Coster). The mpkCCD cells were cultured for 5 days, with daily changes of the medium. FMP-API-1/27, Luteolin (Sigma-Aldrich Corporation), Quercetin (Sigma-Aldrich Corporation), Naringenin (Sigma-Aldrich Corporation), Epicatechin (Sigma-Aldrich Corporation), Pelargonidin (Sigma-Aldrich Corporation), Genistein (Sigma-Aldrich Corporation), or dDAVP was applied to the basolateral side of the mpkCCD cells. FMP-API-1/27 was synthesized as previously described (37). All reagents were dissolved in DMSO. HEK293T cells were cultured on 6-cm diameter dishes in Dulbecco's modified Eagle's medium supplemented with 10% fetal bovine serum. Plasmid DNA was transfected into HEK293T cells using Lipofectamine 2000 reagent (Invitrogen Corporation, Carlsbad, CA). FMP-API-1/27, forskolin (Sigma-Aldrich Corporation), or dDAVP was added to HEK293T for 1 h.

Generation of anti-LRBA antibody.
Plasmid of GST-mouse LRBA (amino acid (AA) 1555-1795) was generated by polymerase chain reaction (PCR) using cDNA of C57BL/6J mice kidney as a template and subsequent insertion of a PCR product into a pGEX-6P-1 vector (GE Healthcare Life Sciences, Chicago, IL, USA). E. coli BL21 (DE3) was transformed with this plasmid, and the GST fusion protein was generated. This fusion protein was purified using a column of glutathione Sepharose Beads (Glutathione Sepharose 4B, Cytiva, Tokyo, Japan). For the cleavage of an N-terminal GST tag, the purified protein was treated with PreScission protease (GE Healthcare) according to the manufacturer's instructions. Rabbits were immunized by this protein four times to generate LRBA antibody. Antibody was purified from the serum by antigen-affinity purification using LRBA (AA1555-1795) purified protein.

Western blot analysis.
The mpkCCD cells were washed twice with phosphate-buffered saline (PBS) and then solubilized in 200 μL of lysis buffer as previously described (37). After centrifugation at 15,000 ×*g* for 10 min at 4 °C, the protein concentration was measured by the Bradford protein assay method (Expedeon Inc., San Diego, CA, USA). The supernatants were denatured in sodium dodecyl sulfate (SDS) sample buffer (Cosmo Bio, Co., Ltd., Tokyo Japan) for 20 min at 60 °C. Whole homogenates of mouse kidneys without the nuclear fraction (600 ×*g*) were prepared, and the crude membrane fraction (17,000 ×*g*) was used to evaluate AQP2 and other proteins as previously described (3). Equal amounts of protein were separated by SDS-PAGE, transferred to nitrocellulose membranes (GE Healthcare), and subjected to immunoblotting. Western blot analysis was performed with the following primary antibodies: goat anti-AQP2 (dilution, 1:1000;

sc-9880; Santa Cruz Biotechnology, Inc., Dallas, TX, USA), rabbit anti-AQP2 (dilution, 1:1000; phospho S256, ab109926; Abcam, Cambridge, UK), rabbit anti-AQP2 (dilution, 1:1000; phospho S261, p112-261; Symansis, Levels, New Zealand), rabbit anti-AQP2 (dilution, 1:1000; phospho S269, p112-269; Symansis), mouse anti-β-actin (dilution, 1:1000; A2228; Sigma-Aldrich Corporation), mouse anti-GAPDH (dilution, 1:1000; #sc-32233; Santa Cruz), rabbit anti-phospho-PKA substrate (dilution, 1:1000; #9624; Cell Signaling Technology, Inc., Beverly, MA, USA), rabbit anti-UT-A1 (dilution, 1:1000; #SPC-406; StressMarq Biosciences, Victoria, BC, Canada), mouse anti-Flag (M2) (dilution, 1:1000; #F3165, Sigma-Aldrich Corporation), rabbit anti-Flag (dilution, 1:1000; #F7425, Sigma-Aldrich), mouse anti-Myc-Tag (dilution, 1:1000; #9B11; Cell Signaling Technology), rabbit anti-HA-Tag (dilution, 1:1000; #C29F4; Cell Signaling Technology), rabbit anti-HaloTag® (#G928A, Promega Corporation), rabbit anti-Albumin (dilution, 1:1000; 16475-1-AP; Proteintech, Chicago, USA), mouse anti-PKA RIIβ (dilution, 1:1000; 610626; BD Biosciences, San Jose, CA, USA), mouse anti-mouse AKAP220 antibody (dilution, 1:1000; 610704; BD Biosciences) and rabbit anti-LRBA (dilution, 1:1000; developed in our laboratory). Alkaline phosphatase-conjugated anti-IgG antibody (Promega Corporation) and goat anti-mouse light chain antibody (AP200A, Sigma-Aldrich) were used as the secondary antibody, and Western Blue (Promega Corporation) was used to detect the signals. The band intensities of the western blots were quantified using ImageJ software (https://imagej.nih.gov/ij/).

Protein purification and mass spectrometry.
dDAVP or vehicle was added to the basolateral side of the mpkCCD cells for 1 h. After treatment, the lysates of mpkCCD cells were collected, as described above. Anti-pPKA substrate antibody (#9624; Cell Signaling Technology) was bound to protein G magnetic beads (Dynabeads® ProteinG, Invitrogen Corporation), and the cell lysates were purified according to the manufacturer's instructions. The proteins bound to the antibody were denatured in an SDS sample buffer (Cosmo Bio, Co., Ltd., Tokyo, Japan) for 20 min at 60 °C. Equal amounts of protein were separated by SDS-polyacrylamide gel electrophoresis and visualized by silver staining (Sil-Best Destain Kit, Nacalai Tesque, Inc. Kyoto, Japan). Two stained bands and their control bands indicated in figure 1D were excised from gels. Liquid Chromatograph - Mass Spectrometry (LC-MS/MS) analysis of gel bands was conducted by MS BioWorks (Ann Arbor, MI, USA) with the following protocol. Each gel was washed with 25-mM ammonium bicarbonate followed by acetonitrile and reduced with 10-mM dithiothreitol at 60 °C, followed by alkylation with 50-mM iodoacetamide at room temperature. The proteins in gels were digested with trypsin (Promega) at 37 °C for 4 h. LC-MS/MS analysis of gel bands was conducted by MS BioWorks (Ann Arbor) with the following protocol. Peptides were loaded on a trapping column and eluted over a 75-μm analytical column at 350 nL/min; both columns were packed with Luna C18 resin (Phenomenex). A 0.5 h gradient was employed. The mass spectrometer was operated in the data-dependent mode, with the Orbitrap operating at 60,000 FWHM and 15,000 FWHM for MS and MS/MS, respectively. Advanced Peak Determination(APD) was enabled, and the instrument was run with a 3-s cycle time for MS and MS/MS. Data were searched using a local copy of Mascot (Matrix Science) with the following parameters: enzyme: trypsin/P; database: SwissProt Mouse (concatenated forward and reverse plus common contaminants); fixed modification: carbamidomethyl (C); variable modifications: oxidation (M), acetyl (N-term), pyroGlu (N-term Q), deamidation (N/Q); Mass values: monoisotopic; peptide mass tolerance: 10 ppm; fragment mass tolerance: 0.02 Da; max missed cleavages: 2. Mascot DAT files were parsed into Scaffold (Proteome Software) for validation, filtering, and creating a non-redundant list per sample. Data were filtered using at 1% protein and peptide false discovery rate (FDR), requiring at least two unique peptides per protein. The mass spectrometry proteomics data have been deposited to the ProteomeXchange Consortium via the PRIDE (4) partner repository with the dataset identifier PXD033852.

Analysis of post-translational modification of LRBA
Myc-LRBA and HA-V2R were overexpressed in HEK293T cells. dDAVP or vehicle was added to the HEK293T cells for 1 h. The cell lysates were purified using anti-c-Myc Magnetic Beads (#88842, Pierce Biotechnology), according to the manufacturer's instructions. The proteins bound to the beads were denatured in an SDS sample buffer (Cosmo Bio, Co., Ltd., Tokyo, Japan) for

20 min at 60 °C. Equal amounts of protein were separated by SDS-polyacrylamide gel electrophoresis and visualized by Coomassie Brilliant Blue Stain One (Nacalai Tesque, Kyoto, Japan). Stained bands were excised from gels. LC-MS/MS analysis of gel bands was conducted by MS BioWorks (Ann Arbor, MI, USA) with the following protocol. Each gel was washed with 25-mM ammonium bicarbonate followed by acetonitrile and reduced with 10-mM dithiothreitol at 60 °C, followed by alkylation with 50-mM iodoacetamide at room temperature. The proteins in gels were digested with trypsin (Promega) at 37 °C for 4 h, and were digested with chymotrypsin or elastase (Promega) overnight at 37 °C. LC-MS/MS analysis of gel bands was conducted by MS BioWorks (Ann Arbor) with the following protocol. Peptides were loaded on a trapping column and eluted over a 75-μm analytical column at 350 nL/min; both columns were packed with Luna C18 resin (Phenomenex). The mass spectrometer was operated in data-dependent mode, with the Orbitrap operating at 60,000 FWHM and 15,000 FWHM for MS and MS/MS respectively. APD was enabled, and the instrument was run with a 3-s cycle for MS and MS/MS. Data were searched using a local copy of Byonic (Protein Metrics) with the following parameters: Enzyme: Trypsin/P or None (Chymotrypsin/Elastase); database: SwissProt Mouse (concatenated forward and reverse plus common contaminants); fixed modification: Carbamidomethyl (C); variable modifications: Acetyl (K), Methyl (K/R), Dimethyl (K), Oxidation (M), Phospho (STY), Trimethyl (K); deamidation (N/Q); mass values: Monoisotopic; Peptide Mass Tolerance: 10 ppm; Fragment Mass Tolerance: 0.02 Da; Max Missed Cleavages: 2 (Trypsin). Byonic mzIdentML files were parsed into Scaffold (Proteome Software) for validation, filtering and to create a non-redundant list per sample. Data were filtered using at 1% protein and peptide FDR and requiring at least two unique peptides per protein. Scaffold results were exported as mzIdentML and imported in to Scaffold PTM in order to assign site localization probabilities using Ascore (S.A. Beausoleil et al. A probability-based approach for high-throughput protein phosphorylation analysis and site localization, Nature Biotechnology 2006, 24, 1285-1292). A minimum localization probability filter of 50% was applied. The mass spectrometry proteomics data have been deposited to the ProteomeXchange Consortium via the PRIDE (4) partner repository with the dataset identifier PXD033859.

Histological analysis.
The mouse kidneys were fixed in 10% formalin neutral buffer solution (Wako, Osaka, Japan). To evaluate renal lymphocyte infiltration, paraffin-embedded sections were stained by the hematoxylin and eosin technique. Histological images were obtained using a BZ-X800 microscope (Keyence, Osaka, Japan).

Immunofluorescence studies.
Mouse kidneys were fixed by perfusion through the left ventricle with 0.2-M periodate lysine and 2% paraformaldehyde in PBS. Tissue samples were soaked for several hours in 20% sucrose in PBS, embedded in Tissue-Tek OCT Compound (Sakura Finetek), and snap-frozen in liquid nitrogen. Goat anti-AQP2 (dilution, 1:500; sc-9882; Santa Cruz), rabbit anti-AQP2 (dilution, 1:200; phospho S269, p112–269; Symansis), rabbit anti-phospho-PKA substrate (dilution, 1:200; #9624; Cell Signaling Technology), and rabbit anti-LRBA (dilution, 1:200; developed in our laboratory) were used as the primary antibody. Alexa 488 and 546 dye-labeled antibodies (dilution, 1:200; Molecular Probes) were used as the secondary antibodies. The samples were mounted with ProLong™ Glass Antifade Mountant with NucBlue™ (P36981, Invitrogen). Immunofluorescence images were obtained using a Leica SP-8 confocal microscope.

Immunoelectron microscopy.
Mouse kidneys were fixed by perfusion solution with 0.2 M periodate lysine and 2% paraformaldehyde in PBS through the left ventricle. The pre-embedding silver enhancement immunogold method was used as previously described (5). Goat anti-AQP2 (dilution, 1:200; sc-9882; Santa Cruz) and rabbit anti-LRBA (dilution, 1:100; developed in our laboratory) were used as the primary antibody.

Double-label immunoelectron microscopy.

Mice were perfused with paraformaldehyde-lysine-periodate (PLP) fixative. The perfused kidneys were cut into small pieces and immersed in the same fixative for about 30 min. The samples were dehydrated with a graded series of ethanol and embedded in LR-white resin (London Resin, Berkshire, UK). 90-nm-thick sections of the LR-white-resin-embedded samples were cut with a diamond knife and transferred to nickel grids (150 mesh) which had been coated with Formvar membrane. After blocking with 1% bovine serum albumin (BSA) in PBS, the sections were incubated with the mixture of the goat-anti-AQP2 (dilution, 1:50; sc-9882; Santa Cruz) and rabbit-anti-LRBA (dilution, 1:50; developed in our laboratory) antibodies diluted with 1% BSA in PBS for 12 h at 4˚C. Subsequently they were incubated with the mixture of colloidal-5-nm-gold-conjugated anti-rabbit IgG (1:100) and 10-nm-gold-conjugated anti-goat IgG (1:100) diluted with 1% BSA in PBS for 1 h at room temperature. The stained sections were fixed with 2.5% glutaraldehyde/0.1 M PBS for 5 min, contrasted with 4% uranyl acetate for 5 min, and observed with a JEM1400Flash transmission electron microscope (JOEL, Tokyo, Japan). The primary antibodies were omitted from the incubation solution as a negative control, and no non-specific staining of the secondary antibody was found in the kidney sections.

Immunoprecipitation.
mpkCCD cell or mouse kidney tissue lysate was incubated with a rabbit anti-LRBA antibody (developed in our laboratory) or a rabbit anti-phospho-PKA substrate antibody (#9624; Cell Signaling Technology, Inc.) captured on protein G magnetic beads (Dynabeads® ProteinG, Invitrogen Corporation) for 1 h at 4 °C. HEK293T cell lysate was incubated with Anti-c-Myc Magnetic Beads (#88842, Pierce Biotechnology) or Anti-FLAG M2 Affinity Gel(#A2220, Sigma-Aldrich Corporation) for 1 h at 4 °C. These protein purifications were performed according to the manufacturer's instructions.

Co-immunoprecipitation *in vivo.*
Whole homogenates of mouse kidneys without the nuclear fraction (600 ×*g*) were prepared, and the crude membrane fraction (17,000 ×*g*) was extracted as previously described (37). Membrane fraction was lysed in lysis buffer containing the following reagents: 250 mM sucrose (Nacalai Tesque), 10 mM triethanolamine (Sigma-Aldrich), 1 mM EGTA (Sigma-Aldrich), 1 mM EDTA (Sigma-Aldrich), 1 mM sodium orthovanadate (Sigma-Aldrich), 50 mm sodium fluoride (Sigma-Aldrich), and 2M Urea (Nacalai Tesque). Lysate was incubated with a mouse anti-PKA RIIβ antibody (610626; BD Biosciences) captured on protein G magnetic beads (Dynabeads® ProteinG, Invitrogen Corporation) for 1 h at 4 °C. These protein purifications were performed according to the manufacturer's instructions.

Quantitative real-time PCR analysis.
Total RNA was extracted using TRIzol Reagent (Invitrogen) and was reverse-transcribed using Omniscript Reverse Transcriptase (Qiagen). Quantitative real-time PCR analysis was performed in a Thermal Cycler Dice Real Time System (Takara Bio). Primers and templates were mixed with SYBR Premix Ex Taq II (Takara Bio). Transcript levels were normalized to GAPDH mRNA levels, and the amount of RNA was calculated using the comparative threshold cycle (CT) method. Primers used for detection of mouse *Aqp2* were 5′-GCC CTG CTC TCT CCA TTG-3′ and 5′-GTT GTC ACT GGC AAG TTT GA-3′, for mouse *Slc14a2* (UT-A1) were 5′- GAC AGT GAG ACG CAG TGA AG-3′ and 5′- ACG GTC TCA GAG CTC TCT TC-3′, for mouse *Akap11* (AKAP220) were 5′- AGG TGG CAG TGG AGA GCT AA-3′ and 5′- GTG CAG AGG GAA GAG TTT CG-3′, for mouse *Akap7* (AKAP7 isoformδ) were 5′- AAG AGG AAG TGG CAC GAG AA-3′ and 5′- TGC TTC TCT TTG GGT TTG CT-3′, and for mouse *Gapdh* were 5′- AAC TTT GGC ATT GTG GAA GG-3′ and 5′- GGA TGC AGG GAT GAT GTT CT-3′.

Plasmids.
mRNA from the mouse kidney was converted into cDNA using Omniscript Reverse Transcriptase. Flag-PKA RIα, Flag-PKA RIβ, Flag-PKA RIIα, Flag-PKA RIIβ, AKAP1-Myc, Myc-AKAP2, and Myc-OPA1 were amplified from the mouse kidney-derived cDNA by PCR, and PCR products were inserted into pcDNA3 using the Gibson assembly technique (New England Biolabs, Ipswich, MA, USA). AVPR2 was subcloned into pTB701HA by the same method. Human HA-CG-NAP

was generated as previously described (6). Myc-hAKAP12, Myc-hARFGEF2, Myc-hMAP2, Myc-hAKAP8, and Myc-hEZR were amplified by PCR using plasmid DNA (Halo-hAKAP12, Halo-hARFGEF2, Halo-hMAP2, Halo-hAKAP8, and Halo-hEZR purchased from Promega Corporation) as templates, and PCR products were inserted into pcDNA3 using the Gibson assembly technique. Halo-hAKAP13, Halo-hCBFA2T3, Halo-hAKAP17A, and Halo-hMSN were purchased from Promega Corporation.

Statistics.
At least three independent experiments were performed to ensure reproducibility. Statistical analyses were performed with JMP14® software (SAS Institute, Inc., Cary, NC, USA) using the two-sided Student's t-tests, Dunnett's test, Tukey test, or Pearson's correlation analysis. Statistical tests of each experiment are shown in the figure legends.

Supplementary Figures and Tables

The amino acid sequence of mouse LRBA

1	masednraps	rpptgddggg	ggkeetpteg	galslkpglp	irgirmkfav	ltglvevgev	snrdivetvf	nllvggqfdl	emnfiiqege	simcmvelle
101	kcdvtcqaev	wsmftailkk	sirnlqvcte	vglvekvlgk	iekvdsmiad	llvdmlgvla	synltvrelk	lffsklqgdk	gqwpphagkl	lsvlkhmpqk
201	ygpdaffnfp	gksaaaialp	piarwpyqng	ftfhtwlrmd	pvnninvdkd	kpylycfrts	kglgysahfv	ggcliitsik	skgkgfqhcv	kfdfkpqkwy
301	mvtivhiynr	wknselrcyv	ngelasygei	twfvntsdtf	dkcflgsset	adanrvfcgq	mtavylfsda	lnaaqifaiy	qlglgykgtf	kfkaesdlfl
401	aehhkllyd	gklssaiaft	ynpratdaql	clesspkdnp	sifvhsphal	mlqdvkavlt	hsiqsamhsi	ggvqvlfplf	aqldykqyls	devdltictt
501	llafimellk	nsiamqeqml	ackgflvigy	slekssksh v	sravlelcla	fskylsnlqn	gmpllkqlcd	hillnpavwi	htpakvqlml	ytylstefig
601	tvniyntirr	vgtvllimht	lkyyywavnp	qdrsgitpkg	ldgprpnqke	ilslraflm	fikqlvmkds	gvkedelqai	lnylltmhed	dnlmdvlqll
701	valmaehpns	mipafdqrng	lrviykllas	ksegirvqal	kalgyflkhl	apkrkaevml	ghglfsllae	rlmlqtnlit	mtmynvlfei	lieqictqvi
801	hkqhpdpdst	vkiqnpqilk	viatllrnsp	qcpesmevrr	aflsdmiklf	nnsrenrrsl	lqcsvwqewm	lslcyfnpkn	sdeqkitemv	yaifrillyh
901	avkyewggwr	vwvdtlsith	skvtfeihke	nlanifreeq	rkgdeetgpc	ssslvpegtg	atrgvdvsvg	sqhedrkdsp	isphftrnsd	enssigrass
1001	idsasntelq	thdmssdekk	verenqelld	qatveetatn	gakddletss	daaepvtins	nslepgkdtv	tisevsasis	spseedaaem	pelleksgve
1101	eeedddyvel	kvegspteea	glptelqgeg	lsvaasegre	epdmcghgce	vqveapitki	hndpettdse	dsrfptvata	gslatssevp	vpqatvqsds
1201	hemldqgmka	tnlagetesv	sdcadnvsea	patseqkitk	ldvssvasdt	erfelkasts	teapqpqrhg	leisrqqeqt	aqqtapdavd	qq rrds rstm
1301	fripefkwsq	mhqrlltdll	fsietdiqmw	rshstktvmd	fvnssdnvif	vhntihlisq	vmdnmvmacg	gilpllsaat	sathelenie	ptqglsieas
1401	vtflqrlisl	vdvlifassl	gfteieaekn	mssggilrqc	lrlvcavavr	nclecqqhsq	lkargdtaks	sktihslipm	gksaakspvd	ivtggispvr
1501	dldrllqdmd	inrlravvfr	diedskqaqf	lalavvyfis	vlmvskyrdi	lepqderhsq	slketssdng	naslpdaent	paefssltls	sveeslegts
1601	ctr rrds glg	eetasglgsg	lsvaspaapl	gvsagpdais	evlctlslev	nksqetridg	gneldrkvtp	svpvsknvnv	kdilrslvnm	padgvtvdpa
1701	llppaclgal	gdlsvdppmq	frsfdrsvii	atkkssvlps	alttsapssa	vsvvssvdpt	hasdtggesp	gsrspnaklp	svaavgsvpq	dpaahmsite
1801	rlehalekaa	pllreifvdf	apflsrtllg	shgqellieg	tslvcmksss	svvelvmllc	sqewqnsiqk	naglafielv	negrllsqm	kdhlvrvane
1901	aefilsrqra	edihrhaefe	slcaqysadk	reeekmcdhl	iraakyrdhv	tatqliqkii	nlltdkhgaw	gssavsrpre	fwrldywedd	lrrrrrfvrn
2001	plgsthpeat	lktavehaad	edilakgkqs	iksqalgnqn	seneallegd	ddtlssvdek	dlenlagpvs	lstpaqlvap	svvvkgtlsv	tsselyfevd
2101	eedpnfkkid	pkilaytegl	hgkwlfteir	sifsrryllq	ntaleifman	rvavmfnfpd	patvkkvvny	lprvgvgtsf	glpqt rris l	atprqlfkas
2201	nmtqrwqhre	isnfeylmfl	ntiagrsynd	lnqypvfpwv	itnyeseeld	ltlpsnfrdl	skpigalnpk	raaffaerfe	sweddqvpkf	hygthystas
2301	fvlawllrie	pfttyflnlq	ggkfdhadrt	fssvsrawrn	sqrdtsdike	lipefyylpe	mfvnfnnynl	gvmddgtvvs	dvelppwakt	seefvrinrl
2401	alesefvscq	lhqwidlifg	ykqqgpeavr	alnvfyylty	egavnlnsit	dpvlreavea	qirsfgqtps	qlliephppr	gsamqasplm	ftdqaqqdvi
2501	mvlkfpsnsp	vthvaantqp	glampavitv	tanrlfavnk	whnlpahqga	vqdqpyqlpv	eidpliacgt	gthrrqvtdl	ldqsiqvhsq	cfvitsdnry
2601	ilvcgfwdks	frvystdtgk	liqvvfghwd	vvtclarses	yiggncyils	gsrdatlllw	ywngkssgig	dnpggetatp	railtghdye	itcaavcael
2701	glvlsgsqeg	pclihsmngd	llrtlegpen	clkpkliqas	reghcvifye	ngcfctfsvn	gklqatvetd	dhirvsavgs	tlfllgssk	

Fig. S1. The amino acid sequence of mouse LRBA isoform beta. Three RRXS motifs are indicated in red.

A

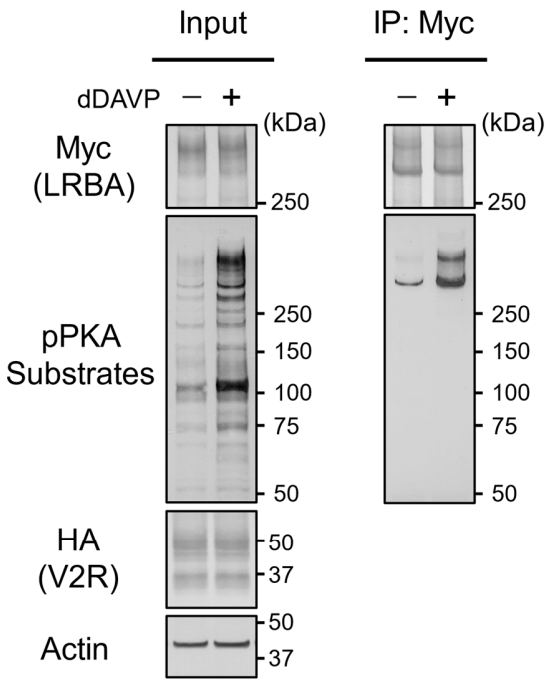

B

Site	Modification	Centralized Sequence	Best Ascore	Localization Probability	Vehicle Modified SpC /Total SpC	dDAVP Modified SpC /Total SpC
S979	Phospho	HEDRKDS*PISPHF	91.01	1	5/34	0/36
S982	Phospho	RKDSPIS*PHFTRN	50.19	0.99999	3/34	1/36
S1000	Phospho	SIGRASS*IDSASN	26.2	0.997517	3/18	2/15
T1117	Phospho	KVEGSPT*EEAGLP	0	0.5	0/8	1/11
S1487	Phospho	GKSAAKS*PVDIVT	1000	1	1/16	2/14
S1607	Phospho	CTRRRDS*GLGEET	78.53	1	0/4	1/3
T1669	Phospho	ELDRKVT*PSVPVS	24.95	0.999949	1/36	0/37
S2189	Phospho	PQTRRIS*LATPRQ	61.87	1	0/13	1/15

Fig. S2. Post-translational modification analysis of LRBA. (**A**) Myc-LRBA and HA-V2R were overexpressed in HEK293T cells. dDAVP (1nM) or vehicle was added to the HEK293T cells for 1 h. Anti-Myc beads were used to perform immunoprecipitation. (**B**) S1607 and S2189 were phosphorylated by dDAVP, while S979 and T1669 were dephosphorylated. SpC: spectral count.

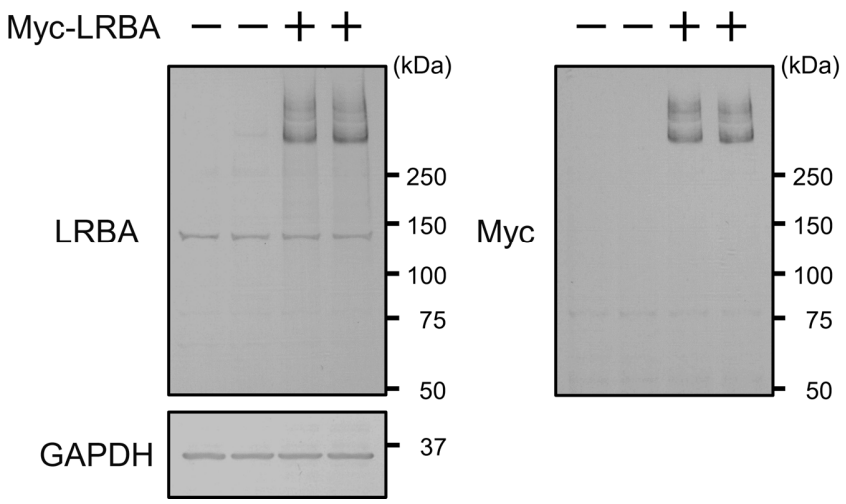

Fig. S3. Validation of anti-LRBA antibody. Representative blots of overexpressed Myc-LRBA in the HEK293T cells (*n* = 3).

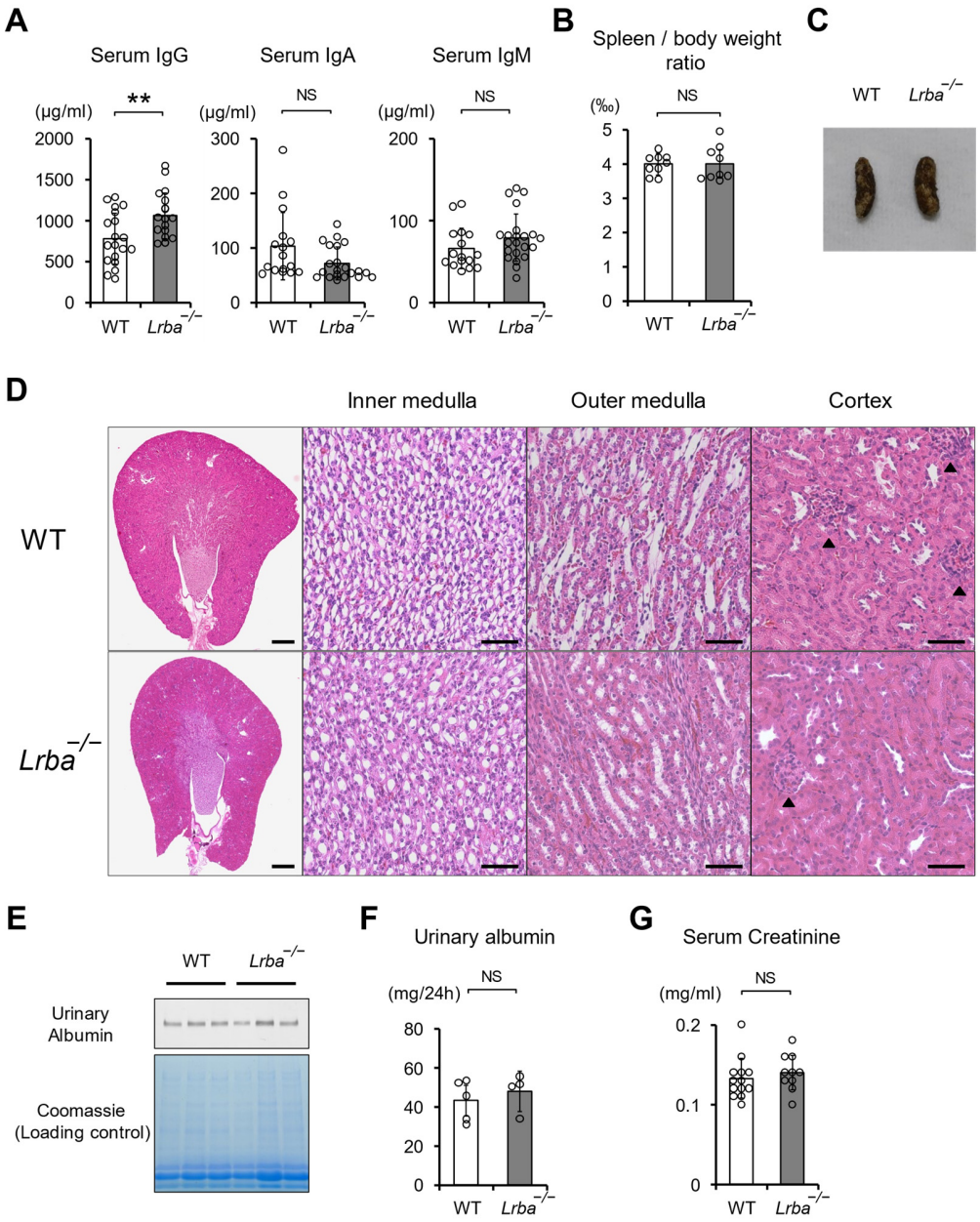

Fig. S4. *Lrba*$^{-/-}$ mice do not show immunological phenotype. (**A**) Serum immunoglobulin levels in *Lrba*$^{-/-}$ mice (IgG; *n* = 19, IgA; *n* = 16/WT, *n* = 21/ *Lrba*$^{-/-}$, IgM; *n* = 16/WT, *n* = 22/*Lrba*$^{-/-}$). (**B**) Spleen weight of *Lrba*$^{-/-}$ mice expressed as a permillage of the total body weight (n = 9). (**C**) The representative stool of *Lrba*$^{-/-}$ mice. (**D**) Hematoxylin and eosin staining shows no histologic abnormalities of the kidney tissue in *Lrba*$^{-/-}$ mice. Arrowheads indicate glomeruli. Scale bars, whole cross section; 500 μm, other panels; 50 μm. (**E**) Urinary albumin of *Lrba*$^{-/-}$ mice. Coomassie is showed as loading control (*n* = 6). (**F**) Albumin excretion in 24 h urine was measured by ELISA (*n* = 5/WT, *n* = 4/*Lrba*$^{-/-}$). (**G**) Serum creatinine levels of *Lrba*$^{-/-}$ mice (*n* = 13/WT, *n* = 10/*Lrba*$^{-/-}$). Data are mean ± SD. Two-sided Student's t-test, $^{**}p < 0.01$, NS: not significant.

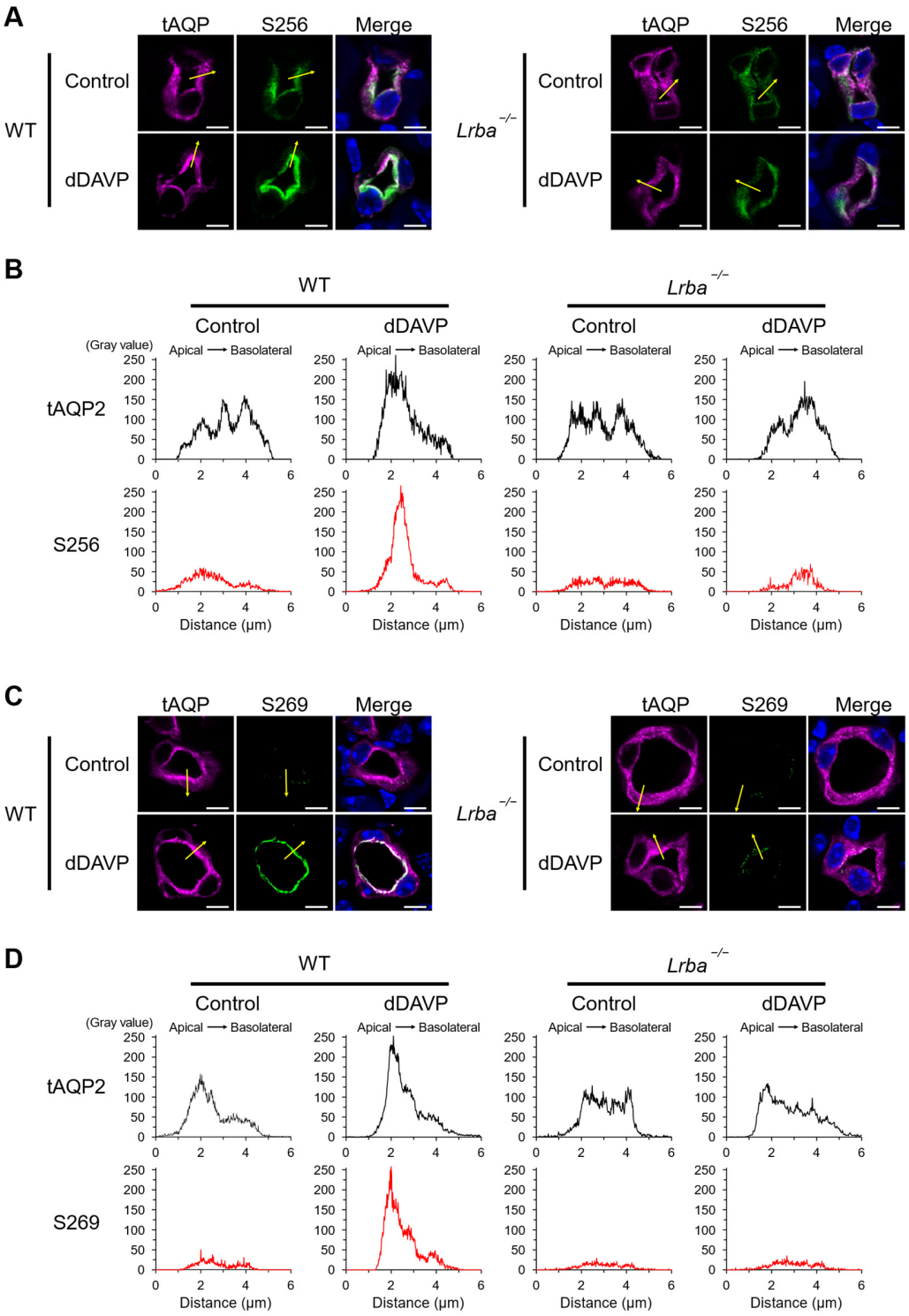

Fig. S5. Fluorescence intensity of AQP2 in Figure 4D and 4E is quantified. (**A** and **B**) Fluorescence intensity of AQP2 and p256-AQP2 at yellow lines was quantified. Scale bars, 5μm. (**C** and **D**) Fluorescence intensity of AQP2 and p269-AQP2 at yellow lines was quantified. Scale bars, 5μm.

The amino acid sequence of mouse UT-A1

1	msdhhplkem	sdsnsspllp	eplssrykly	eselssptwp	sssqdthpal
51	pllempeekd	lrssdedshi	vkiekpnern	k rres evs rr	as agrggfsl
101	fqavsyltgd	mkecknwlkd	kplvlqfldw	vlrgaaqvmf	vnnpisglii
151	figlliqnpw	wtiagtlgtv	astlaalals	qdrsaiasgl	hgyngmlvgl
201	lmavfsekld	yywwllfpvt	ftsmacpiis	salstifakw	dlpvftlpfn
251	ialtlylaat	ghynlffptt	likpasaapn	itwteiempl	llqtipvgvg
301	qvygcdnpwt	ggmilvalfi	sspliclhaa	igsivgllaa	ltvatpfeti
351	ylglwsyncv	lsciaiggmf	yaltwqthll	alvcalfcay	mgaalsntma
401	vvgvpsgtwa	fclstltfll	ltsnntgiyk	lplskvtype	anriyfltvr
451	rseeekspng	gsgeqshgsg	qwkaeesset	vlp rrrs vfh	iewssi rrrs
501	kvfgkgehqe	rqtkeplpcp	yrkptvelfd	ldtmeestei	kveantarts
551	wiqssmvagg	krvskalsyi	tgemkecgeg	lkdkspvfqf	ldwvlrgmsq
601	vmfvnnplsg	ilivlglfvq	npwwailgcl	gtvmstltal	ilsqdksaia
651	aglhgyngvl	vgllmavfsd	kgnyywwlll	pvivmsmtcp	ilssalstvf
701	skwdlpvftl	pfniavtlyl	aatghhnlff	pttllqpttt	ppnitwsdiq
751	vslllraipv	gigqvygcdn	pwtggiflva	lfissplicl	haaigstigm
801	laalsiatpf	dsiyfglcgf	nstlaciaig	gmfyvitwqt	hllaiacalf
851	aaylgaalan	mlsvfglppc	twpfclsalt	flllltsnnpa	iyklplskvt
901	ypeanriyfl	sqekn rras t	itkyqaydvs		

The amino acid sequence of mouse AQP2

1	mwelrsiafs	ravlaeflat	llfvffglgs	alqwasspps	vlqiavafgl
51	gigtlvqalg	hvsgahinpa	vtvaclvgch	vsflraafyv	aaqllgavag
101	aailheitpv	eirgdlavna	lhnnatagqa	vtvelfltmq	lvlcifastd
151	errsdnlgsp	alsigfsvtl	ghllgiyftg	csmnparsla	pavvtgkfdd
201	hwvfwigplv	gavigsllyn	yllfpstksl	qerlavlkgl	epdtdweere
251	vrrrqsvelh	spqslprgsk	a		

Fig. S6. The amino acid sequence of mouse UT-A1 isoform a and mouse AQP2. RRXS motifs are indicated in red.

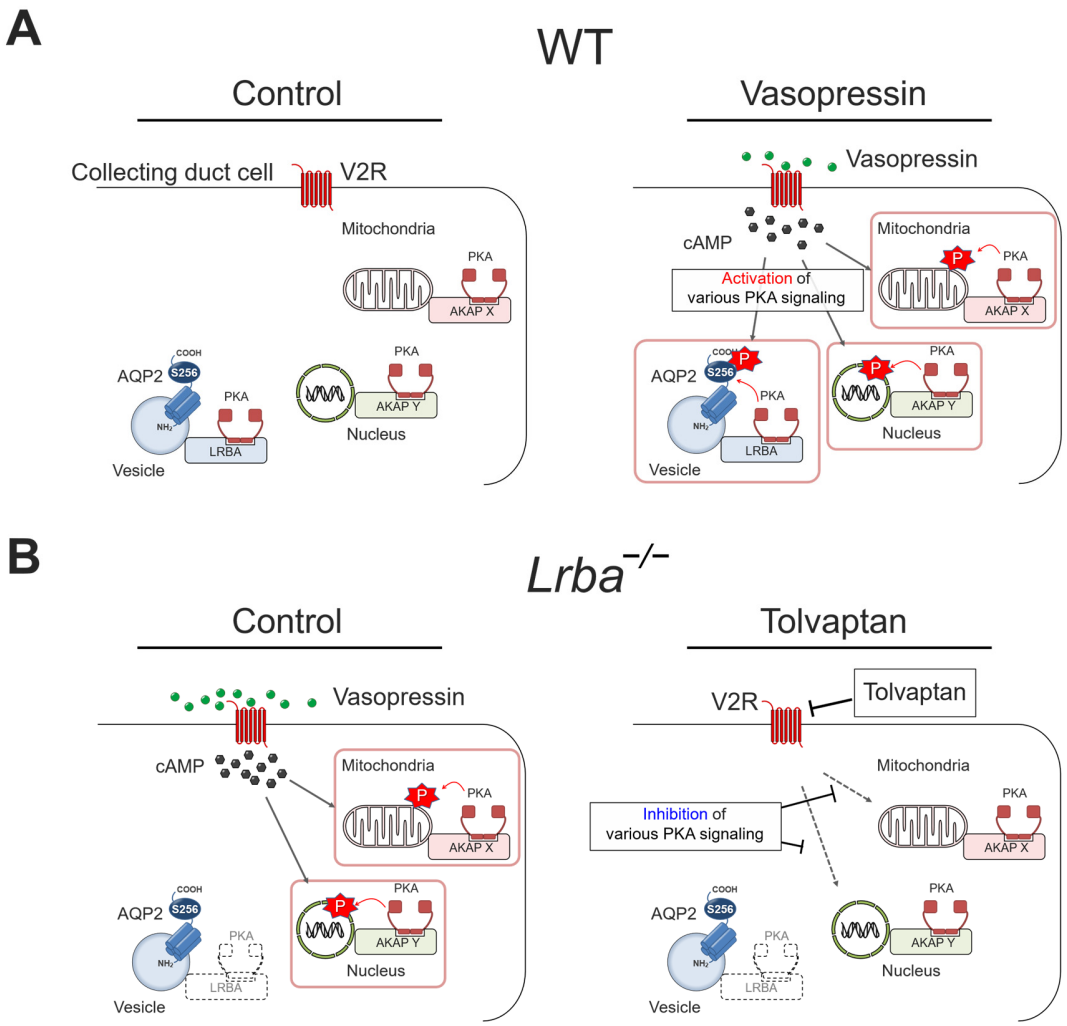

Fig. S7. A schematic summary of the inhibitory effects of tolvaptan on phosphorylation of PKA substrates in *Lrba*$^{-/-}$ mice. (**A**) Left, AKAPs serve as subcellular "address tags". Each AKAP creates compartmentalized PKA signaling to ensure substrate specificity of PKA. Right, vasopressin activates various PKA signaling in renal collecting ducts. (**B**) Left, compensatory elevation in serum vasopressin levels in *Lrba*$^{-/-}$ mice activates various PKA signaling except LRBA-mediated PKA signaling. Right, tolvaptan inhibits vasopressin-induced phosphorylation of PKA substrates mediated by AKAPs other than LRBA.

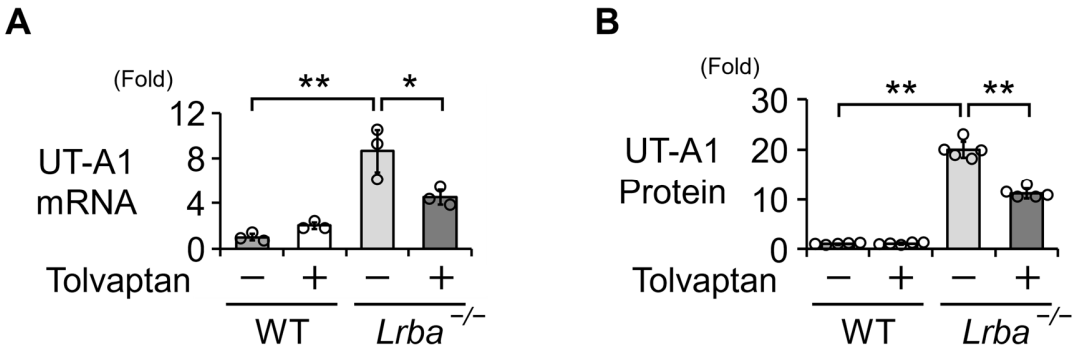

Fig. S8. Tolvaptan decreases mRNA and protein expressions of UT-A1. (**A**) UT-A1 mRNA levels are quantified by qPCR (n = 3). (**B**) Densitometric analysis of UT-A1 protein expression (n = 5). Data are mean ± SD. Tukey test, *$p < 0.05$, **$p < 0.01$.

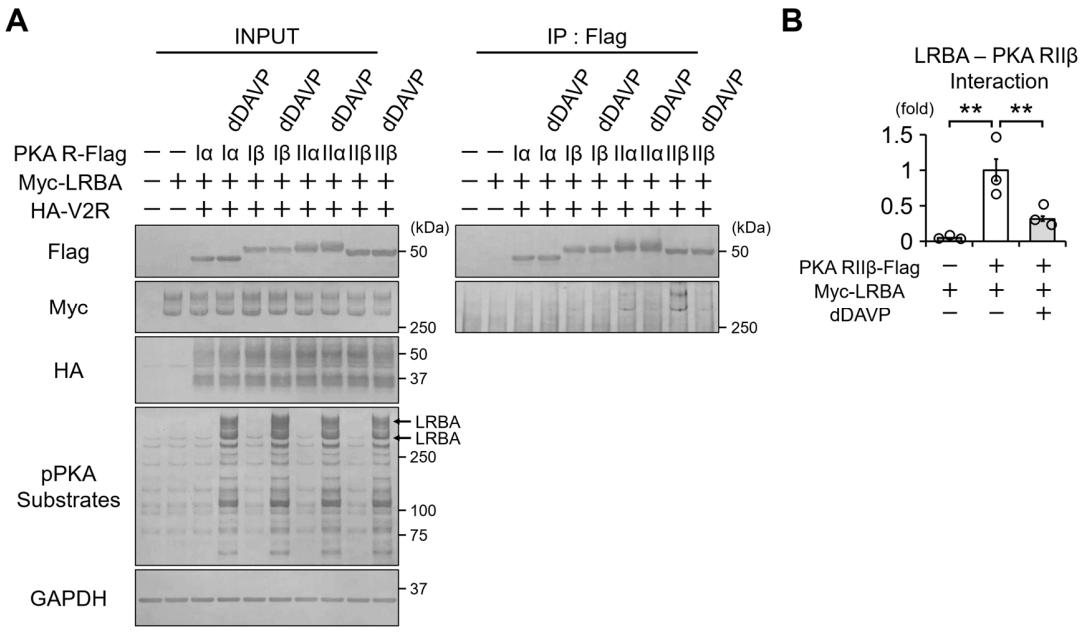

Fig. S9. Vasopressin dissociates the LRBA–PKA RIIβ interaction. (A and **B)** PKA regulatory subunits (RIα, RIβ, RIIα, RIIβ)-Flag, Myc-LRBA, and HA-V2R were overexpressed in the HEK293T cells. dDAVP (1 nM) was added to the HEK293T cells 1 h before co-immunoprecipitation. (**A**) Representative blots are shown. (**B**) Densitometric analysis of co-immunoprecipitated Myc-LRBA (n = 3). Data are mean ± SD. Tukey test, $^{**}p < 0.01$.

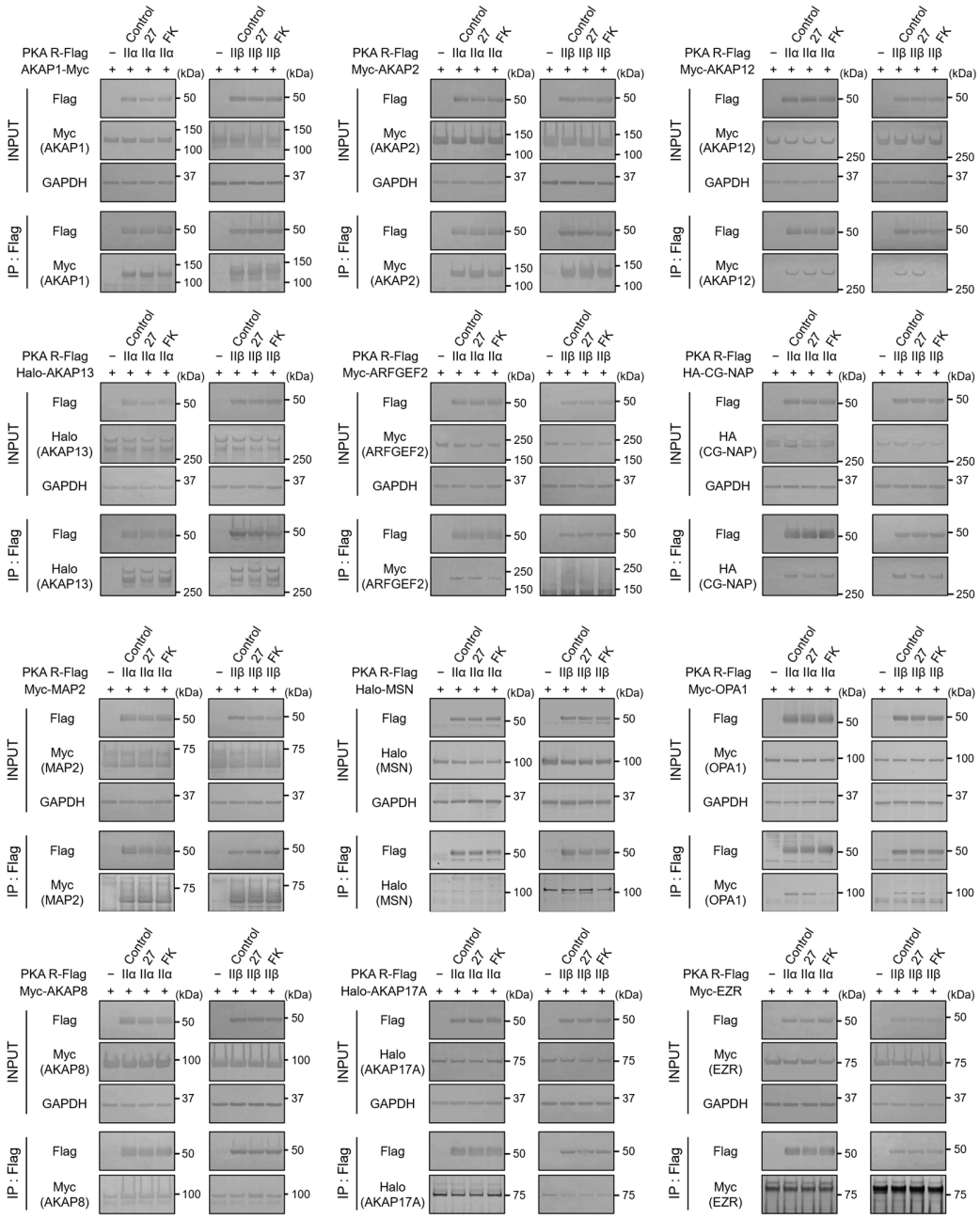

Fig. S10. Co-immunoprecipitation assay for measuring AKAP–PKA interactions. PKA RII subunits (RIIα, RIIβ)-Flag and AKAPs (AKAP1-Myc, Myc-AKAP2, Myc-AKAP12, Halo-AKAP13, Myc- ARFGEF2, HA-CG-NAP, Myc-MAP2, Halo-MSN, Myc-OPA1, Myc-AKAP8, Halo-AKAP17A, and Myc-EZR) were overexpressed in HEK293T cells. FMP-API-1/27 (200 μM) or forskolin (10 μM) was added to the HEK293T cells for 1 h. Anti-Flag beads were used to perform co-immunoprecipitation. Representative blots are shown (n = 3).

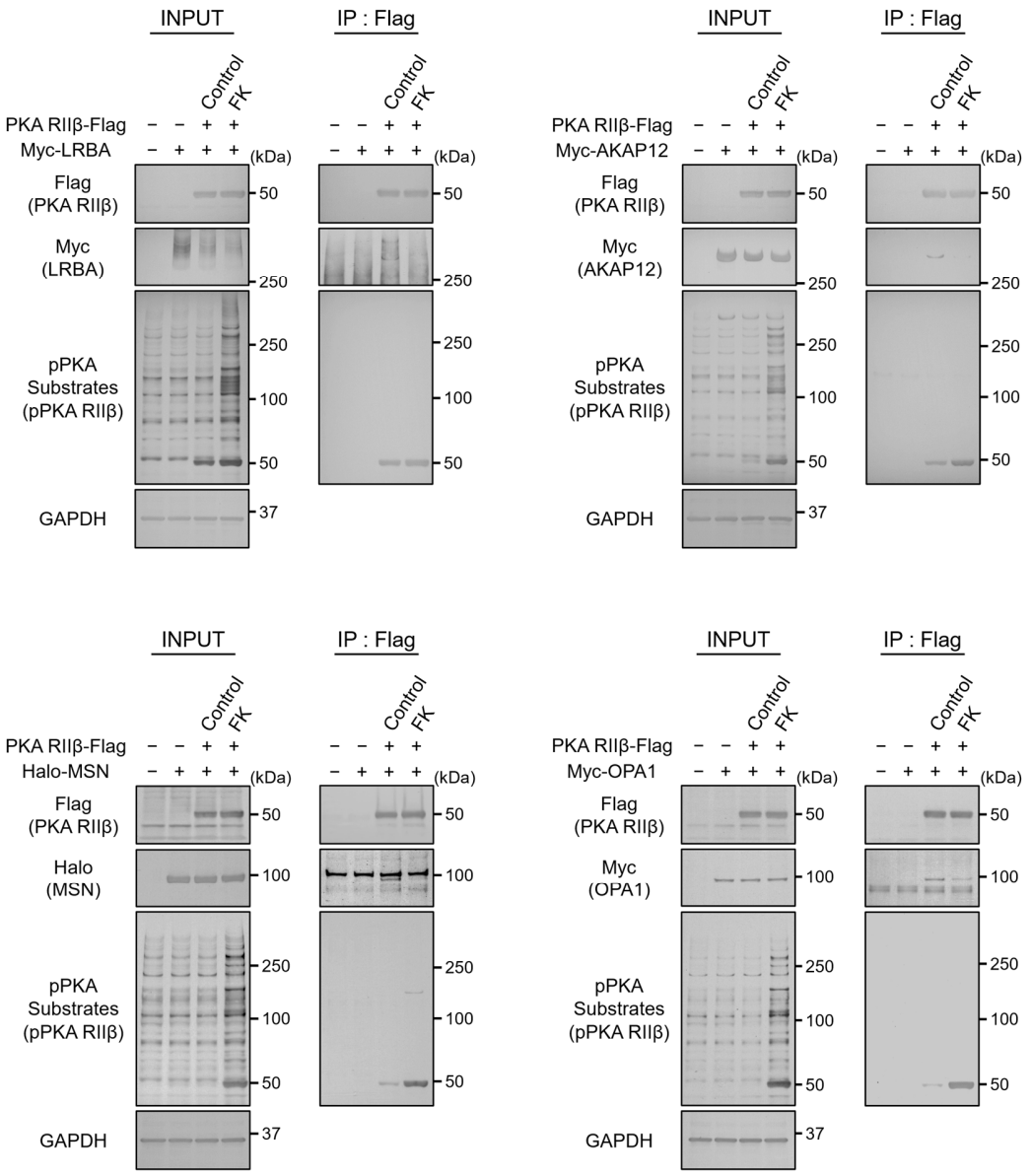

Fig. S11. LRBA–PKA RIIβ, AKAP12–PKA RIIβ, MSN–PKA RIIβ, and OPA1–PKA RIIβ interactions are dissociated by forskolin in spite of phosphorylation at PKA RIIβ. PKA RIIβ-Flag, Myc-LRBA, Myc-AKAP12, Halo-MSN, and Myc-OPA1 were overexpressed in HEK293T cells. Forskolin (10μM) was added to the HEK293T cells for 1 h. Anti-Flag beads was used to perform co-immunoprecipitation. Representative blots are shown (*n* = 3).

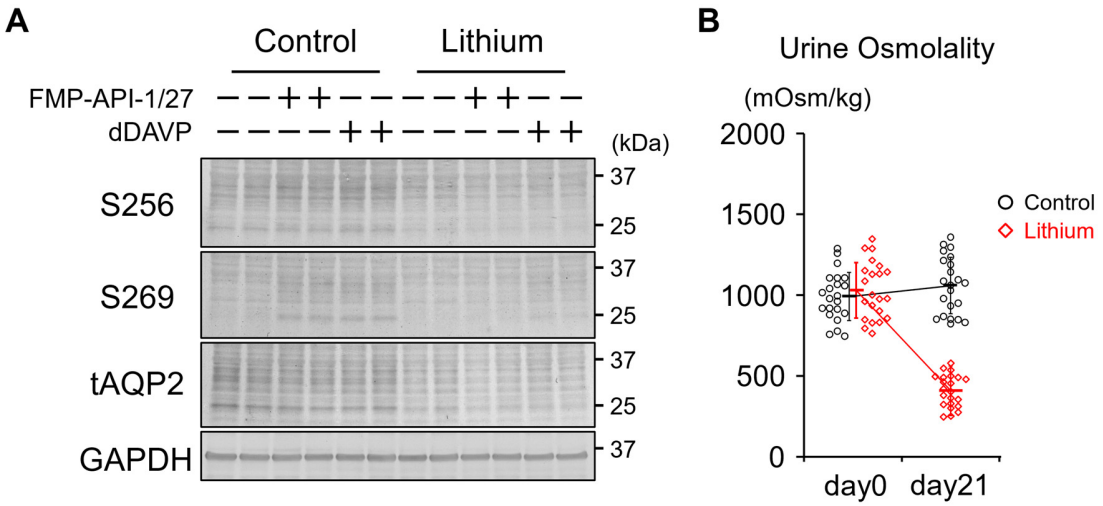

Fig. S12. The effects of FMP-API-1/27 on a lithium-induced diabetes insipidus mouse model. (**A**) AQP2 expression levels are decreased by LiCl. Mice were fed a control diet or a diet containing 0.2% LiCl for 21days. FMP-API-1/27 (30 mg/kg), dDAVP (0.4 μg/kg) or vehicle was intraperitoneally injected into mice for 1 h (*n* = 6). (**B**) Chronic lithium treatment leads to a decrease in urine osmolality. Urine osmolality at the beginning and end of the experiments (*n* = 22). Data are mean ± SD.

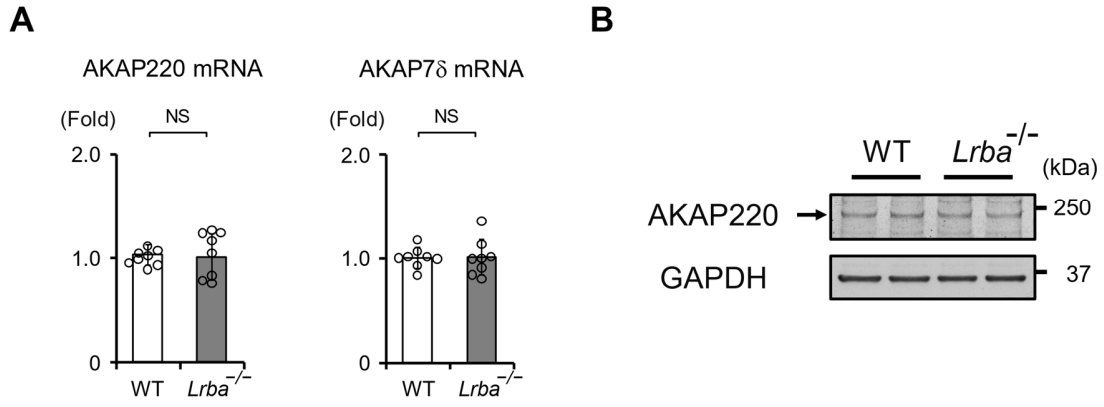

Fig. S13. AKAP220 and AKAP7δ expression levels are not changed in *Lrba*$^{-/-}$ mice. (**A**) AKAP220 and AKAP7δ mRNA expression levels are not different between WT and *Lrba*$^{-/-}$ mice. mRNA levels were quantified by qPCR (*n* = 8). (**B**) AKAP220 protein expression levels in *Lrba*$^{-/-}$ mice are not changed. Representative blots are shown (*n* = 6). (**A**) Two-sided Student's t-test, NS: not significant

AKAPs	RRXS/T	RKXS/T	KRXS/T	KKXS/T	RXS/T
Ezr	1	0	1	2	3
Msn	0	1	0	3	4
Akap2	1	0	0	1	6
Opa1	0	1	0	0	5
Lrba	3	2	0	1	14
Acbd3	0	0	0	0	0
Akap8	0	0	0	1	2
Arfgef2	2	0	0	0	8
AKAP17A	5	2	0	0	9
Akap9(CG-NAP)	2	6	1	2	22
Map2	4	2	2	2	15
Akap10	0	0	0	1	5
Pde4dip	0	1	0	1	17
Nf2	0	0	1	2	6
Akap13	2	1	3	4	27
Chd8	2	2	3	2	16
Akap1	2	0	0	0	6
Akap7	0	0	1	2	2
Synm	2	0	2	0	21
Myo7a	0	2	0	2	12
Rab32	0	0	0	0	2
Akap12	1	3	0	2	6
Akap11	0	0	0	0	2
Akap3	0	0	0	0	4
Akap4	0	0	0	1	4
Akap5	1	1	0	2	7
Akap6	1	1	4	4	19
Akap14	0	0	0	0	2
Akap17b	1	0	1	1	6
Cmya5	2	4	2	0	26
Gskip	0	0	0	0	0
Itga4	1	0	1	0	6
Myrip	0	0	0	1	8
Nbea	1	0	0	0	14
Pik3cg	1	0	0	2	6
Rsph3	1	0	0	0	4
Runx1t1	1	1	1	0	9
Sphkap	3	0	0	1	19
Tnnt2	0	0	1	0	2
Wasf1	0	0	0	0	5
Cbfa2t3	0	1	1	0	6

Table. S1. The number of PKA substrate consensus motifs ([RK] [RK]–X–[ST] and [R]–X–[ST]) in each AKAP.

References

1. T. Rieg *et al.*, Vasopressin regulation of inner medullary collecting ducts and compensatory changes in mice lacking adenosine A1 receptors. *Am J Physiol Renal Physiol* **294**, F638-644 (2008).
2. F. Ando *et al.*, Wnt5a induces renal AQP2 expression by activating calcineurin signalling pathway. *Nat Commun* **7**, 13636 (2016).
3. S. S. Yang *et al.*, Molecular pathogenesis of pseudohypoaldosteronism type II: Generation and analysis of a Wnk4(D561A/+) knockin mouse model. *Cell Metabolism* **5**, 331-344 (2007).
4. Y. Perez-Riverol *et al.*, The PRIDE database resources in 2022: a hub for mass spectrometry-based proteomics evidences. *Nucleic Acids Res* **50**, D543-D552 (2022).
5. N. Tamura *et al.*, Differential requirement for ATG2A domains for localization to autophagic membranes and lipid droplets. *FEBS Lett* **591**, 3819-3830 (2017).
6. M. Takahashi *et al.*, Characterization of a novel giant scaffolding protein, CG-NAP, that anchors multiple signaling enzymes to centrosome and the Golgi apparatus. *Journal of Biological Chemistry* **274**, 17267-17274 (1999).